Winter 2-28-2013

Measuring material relaxation and creep recovery in a microfluidic device

Alison E. Patteson (Koser)
University of Pennsylvania

Lichao Pan
University of Pennsylvania

Nathan C. Keim
University of Pennsylvania

Paulo E. Arratia
University of Pennsylvania

Lab on a Chip

RSC Publishing

TECHNICAL INNOVATION

View Article Online
View Journal | View Issue

Measuring material relaxation and creep recovery in a microfluidic device

Cite this: *Lab Chip*, 2013, **13**, 1850

Alison E. Koser, Lichao Pan, Nathan C. Keim and Paulo E. Arratia*

We present a novel method of testing creep recovery in a microfluidic device. This method allows for the measurement of relaxation time of fluids at low strain. After applying a steady pressure-driven flow along a microchannel, the pressure is released and the fluid is allowed to relax and come to rest. Local strains are observed *via* the time-dependent velocity profiles and are fit to a general viscoelastic model to obtain the fluids' relaxation times. The use of polymeric solutions of various molecular weights allows for the observation of time scales for strains ranging from 0.01 to 10. Results are consistent with data obtained in a macroscopic rheometer and with a viscoelastic constitutive model.

Received 14th December 2012,
Accepted 28th February 2013

DOI: 10.1039/c3lc41379a

www.rsc.org/loc

Many fluids of practical interest for lab-on-a-chip devices contain polymers, cells, or solids and exhibit non-Newtonian behavior. Examples include polymeric solutions, DNA suspensions, foams, and human blood. An important feature of many non-Newtonian fluids is that they often exhibit viscoelasticity.[1,2] In such fluids, the mechanical stresses are history-dependent and rely on a characteristic time λ that in dilute solutions is proportional to the relaxation time of a single polymer molecule or cell, for example.[1,2] In semi-dilute solutions, λ depends also on molecular interactions. These stresses grow nonlinearly with strain rate and can dramatically change the flow behavior in microfluidic devices.[3–10] A common challenge in rheology is to reliably measure the viscoelastic properties, such as λ, of fluids at low strains and for fluids with small, but finite amounts of elasticity.[11]

The viscoelastic response of fluids generally depends on the time scale at which the sample is probed.[1] Viscoelastic properties (*e.g.* λ) are usually measured under time-dependent or dynamic conditions in macroscopic rheometers by imposing a known stress or strain. The shortest accessible time scale is limited by the onset of inertial effects, when the oscillatory shear wave decays appreciably before propagating throughout the entire sample. If the shear strain amplitude is small, the structure is not significantly deformed and the material remains in equilibrium, leading to inaccurate measurements. Microfluidics offers an exciting alternative for measuring the viscoelastic properties of fluids. The exquisite flow control of microfluidic devices allows for precise manipulation of the applied stresses to the fluid sample, which are determined by applied pressures and channel geometry, unlike force transducers in macroscopic rheometers which can be expensive and lack resolution at small strains. The use of high-speed cameras and high-power microscopy allows for extremely precise resolution in both time and space. Furthermore, at small length scales, the Reynolds number remains low even at high strain rates, avoiding inertial instabilities. The Reynolds number Re is the ratio of inertial to viscous forces and is usually defined as $\mathrm{Re} = \rho UL/\mu$, where μ and ρ are fluid viscosity and density, U is mean fluid velocity, and L is a characteristic length scale. To date, a number of methods have successfully measured material properties, such as viscosity, yield stress, and shear-thinning exponents in microfluidic devices.[12–15]

Most of that previous work, however, has focused on steady-state rheology.[3–10,12,14] With few exceptions,[16,17] the dynamic viscoelastic properties of fluids have not been measured in microfluidic devices. And although steady-state rheology is of fundamental importance, there are many microfluidic operations in which time-variant flows are the norm including mixing,[18] pumping,[19] and sorting.[20,21] Here, we present a creep recovery test in a microfluidic device capable of measuring the relaxation time (λ) of fluids. Our method is simple and cost-effective and can use equipment found in most laboratories. Furthermore, the flow-through operation of the device continually renews the sample. This minimizes the degradation of often-fragile samples during experiments because the time spent at high shear-rates is relatively small compared to batch operations such as cone-and-plate rheometry. The working principles are demonstrated with both Newtonian and viscoelastic fluids. Our experiments can make sensitive measurements at time scales of 20 ms at strains as small as 0.01. Thus, this method has potential applications for numerous biological materials, including dilute polymeric solutions in which small time scales at low strain are difficult to measure.

The microfluidic device consists of a square microchannel, a constant-pressure source, a pneumatic valve, and two reservoirs, as shown schematically in Fig. 1. The microchannel is made of polymethyl methacrylate (PMMA) and is 500 μm

Department of Mechanical Engineering and Applied Mechanics, University of Pennsylvania, Philadelphia, PA 19104, USA. E-mail: parratia@seas.upenn.edu

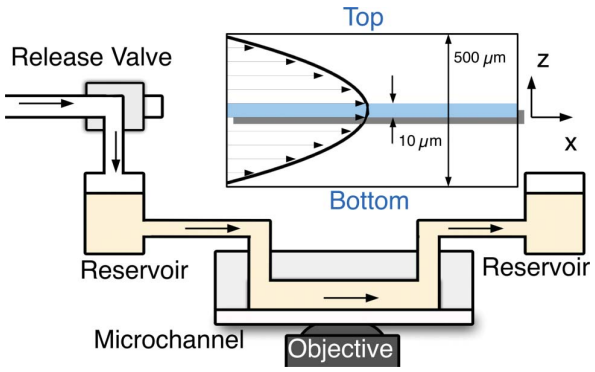

Fig. 1 Experimental setup schematic. Pressurized air drives fluid through a microfluidic channel. A pneumatic valve outside of the channel rapidly releases the applied pressure. Balancing the inlet and outlet fluid heights ensures there is no gravity-driven flow. Velocity profiles are measured at the center plane of the channel.

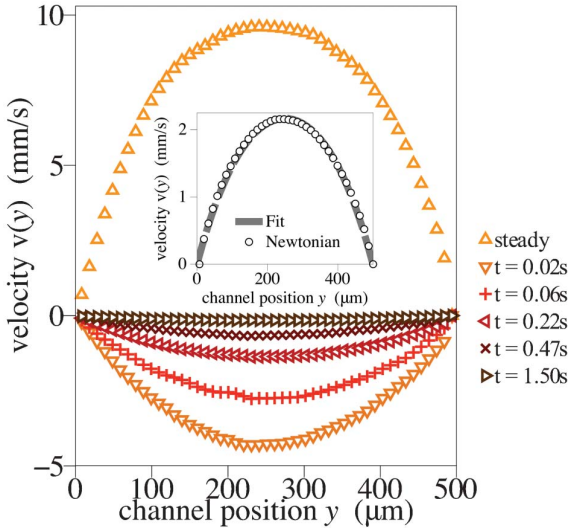

Fig. 2 Velocity profiles of the PAA solution with MW 1.8 × 10^7 at different times. The inset plots the steady velocity profile for the Newtonian fluid and is overlaid with the analytical solution. For the PAA solution, flow is initially positive, but rapidly reverses direction when the applied pressure is released. Velocity profiles approach zero over time as the fluid relaxes.

deep, 500 μm wide, and 3 cm long. The microchannel is sealed with optically clear tape. The channel is connected to a constant-pressure air supply, in this case a pressure-controlled pump (Eppendorf, 920010504), which sustains a prescribed pressure drop across the length of the channel. This applied pressure drop can be rapidly released by opening the pneumatic valve (Parker, 912-000001-003). Particle tracking velocimetry methods are used to obtain velocity profiles of both viscoelastic (Fig. 2) and Newtonian (Fig. 2, inset) fluids. We find that for a Newtonian fluid, the flow stops almost instantaneously once the pressure drop is removed (Fig. 3a). However, for a viscoelastic fluid, there is an observable material relaxation (Fig. 3). Here, we show that this material relaxation can be reliably quantified (Fig. 4).

Both Newtonian and viscoelastic fluids are used in this work. The Newtonian fluid is a 96% glycerol aqueous solution of viscosity $\mu \approx 0.6$ Pa s. Viscoelasticity is investigated by preparing dilute polymeric solutions of various molecular weight (MW) so that different levels of elasticity can be studied. The polymer used is polyacrylamide (PAA), a linear molecule with a flexible backbone. We use molecular weights of: 1.5 × 10^3, 1.0 × 10^4, 1.0 × 10^6, 5.0 × 10^6 and 1.8 × 10^7. The overlap concentration c^* for these MWs are 4.5 × 10^5, 1.0 × 10^5, 3400, 1300, and 350 ppm, respectively. We choose concentrations in the dilute regime such that $c/c^* = 0.3$ for each MW. The polymer is then dispersed in a viscous Newtonian solution of 90% glycerol and 10% DI water. In this way, the elasticity increases with MW, while the shear viscosity remains roughly constant ($\approx$0.3 Pa s).[7]

The creep recovery test in the microchannel begins by applying an initial (shear) stress and allowing the sample to flow steadily, then rapidly releasing the pressure. The ensuing material response is measured as a time- and position-dependent strain, computed from velocity measurements during the entire pressure release process. The strain is fit to a general viscoelastic model undergoing elastic recoil due to cessation of a steady shear stress.

For all fluids, the applied shear stress (τ) is determined by a force balance, $\tau = \frac{\Delta P}{L} y$, where here y is the distance from the center of the channel and ΔP is the pressure drop across the length (L) of the channel.[12,14] In this way, the initial shear stress can be calculated from the controlled pressure drop. At $t = 0$, the applied pressure drop is released and the shear stress rapidly approaches zero (within 10 ms). Next, we measure the velocity profiles $v(y,t)$ as a function of channel position y and time t using particle tracking methods. The fluid is seeded with small fluorescent particles (3 μm in diameter) that are tracked using a CMOS camera and an epi-fluorescent microscope. The images are taken at 2000 frames per second to ensure that one particle moves a distance less than the distance between two adjacent particles between consecutive frames. The particle tracks are measured at a mid-plane between the top and bottom walls of the channel in order to minimize the effects of out-of-plane velocity gradients (Fig. 1); the thickness of the measuring plane is approximately 10 μm. The measured particle tracks are then used to compute the velocity profiles.

Fig. 2 shows velocity profiles for a polymeric solution (MW = 1.8 × 10^7) and the Newtonian fluid (Fig. 2 inset). The inset shows that the Newtonian velocity profile is nearly parabolic and it is well captured by the analytical solution. The viscoelastic data show a nearly-parabolic profile even as it relaxes to zero flow. Furthermore, the flow reverses direction once pressure is released ($t = 0$); the fluid velocity approaches zero over the fluid relaxation time λ. The velocity profiles $v(y,t)$ are used to compute the shear rate $\dot{\varepsilon}(y,t)$ as $\dot{\varepsilon}(y,t) = \frac{\partial v(y,t)}{\partial y}$. The strain $\varepsilon(y,t)$ is then defined as $\varepsilon(y,t) = \int_0^t \dot{\varepsilon}(y,t')\mathrm{d}t'$, which will be denoted as $\varepsilon(t)$ from now on. We can also define the recoverable

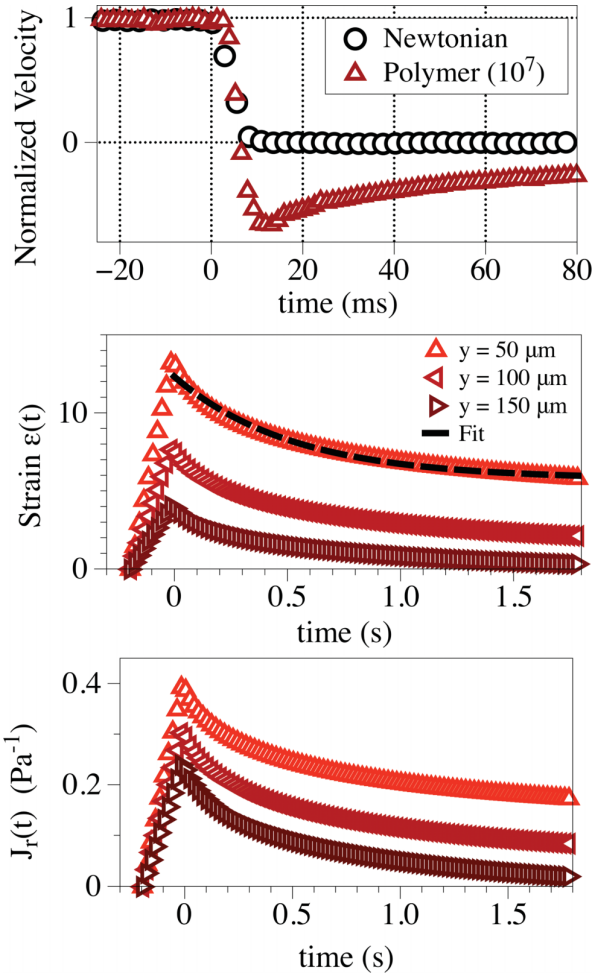

Fig. 3 (a) Normalized velocity at the center of the channel *versus* time for a Newtonian fluid and a PAA solution. (b) Strain *versus* time for different channel positions *y* for a PAA solution with MW 1.8×10^7. We fit the recovery portion, the region where $t > 0$, to eqn (1). (c) Recoverable creep $J_r(t)$ for different channel positions.

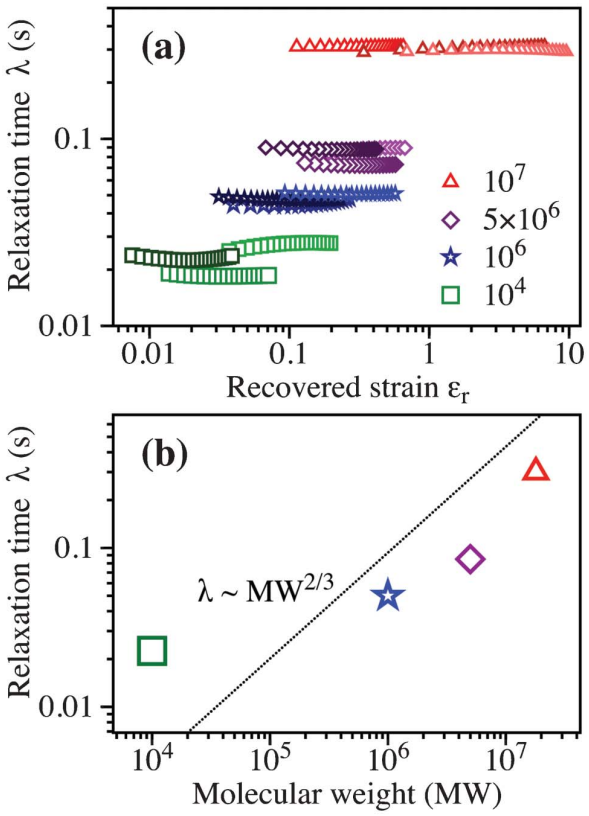

Fig. 4 (a) Fluid relaxation time λ *versus* recovered strain ε_r for all polymeric solutions. Symbols are labeled by MW. (b) Averaged λ *versus* polymer MW shows scaling consistent with FENE model.

creep function as $J_r = \varepsilon(t)/\tau_0$, where τ_0 is the initial shear stress. Note that the shear stress, shear rate, and strain all depend on the channel position *y*. Thus, for any fixed pressure drop across the length of the channel, we apply a range in stress and likewise measure a range in shear rates and strain.

Fig. 3a shows the time-resolved average velocity $\tilde{v}(y,t)$ along a streamline (fixed *y*) for a polymeric solution (MW = 1.8×10^7) and the Newtonian fluid as the pressure is released. Also shown in Fig. 3b and 3c are the strain $\varepsilon(y,t)$ and recoverable creep function $J_r(t)$ for the same polymeric solution. The relaxation time λ is then calculated by fitting the strain data to a general viscoelastic model undergoing the cessation of a steady shear stress, which is a well-known calculation.[2] The solution is of the form

$$\varepsilon(t) = \varepsilon_0 e^{-t/\lambda}. \quad (1)$$

Note that a more specific model such as the Jeffrey model or the Kelvin–Voigt model, under the same specified conditions, will also result in the exponential form of strain as shown in eqn (1). However, since any generalized viscoelastic model results in approximately this form of strain,[2] our measurement does not require more detailed modeling, which can be challenging for complex fluids.

The values of λ measured in our device are shown in Fig. 4. The strain data are fit from $t = 0$, where ε is at a maximum, until a time t_∞, where ε remains roughly constant. The time t_∞ is chosen such that $\dot{\varepsilon}(t = t_\infty)/\dot{\varepsilon}(t = 0)$ is less than 0.05.

In this work, we test the feasibility of measuring time-dependent behavior of viscoelastic fluids using a simple microfluidic device. We have shown that once the applied pressure drop is released, the flow of Newtonian fluids stops. In viscoelastic materials, however, we observe tracer particles rapidly reversing direction, and then coming to rest over the time scale of the fluid. In Fig. 3a, the normalized center velocity *versus* time is plotted for both the Newtonian fluid and the PAA solutions. For the Newtonian case, the time necessary for the applied pressure to be released is approximately 10 ms. This time scale is set by the time it takes for the pneumatic valve to completely open. A very different behavior is observed for the case of a polymeric solution (PAA, MW = 1.8×10^7), as shown in Fig. 3a. Flow reversal and a much longer approach to zero flow are observed for the polymeric solution (Fig. 3a).

Strain curves $\varepsilon(t)$ (Fig. 3b) and recoverable creep $J_r(t)$ (Fig. 3c) for all polymeric solutions are computed from the time-dependent velocity profiles (Fig. 2) and the method discussed above. The quantities $\varepsilon(t)$ and $J_r(t)$ can be computed at various channel positions y. We find that both quantities show an approximately exponential decay with time.

The polymeric solution's relaxation λ is computed by fitting the strain data to the general viscoelastic model (eqn (1)). Fig. 4a shows the values of λ as a function of recovered strain. Here, the recovered strain ε_r is defined as the difference between the maximum strain value and the strain value as $t \rightarrow \infty$. These tests are conducted at initial ΔP values of 5, 10, and 20 kPa. The overlap of λ for each MW of different initial pressure drops assures reproducibility and defines the level of uncertainty. We also find that the time scale is nearly independent of strain (Fig. 4a). The lowest measured time scale is 20 ms for the fluid with MW 1.0×10^4. However, in Fig. 4a, we see an increase in noise for this fluid, marking the lower end of the device resolution consistent with the 10 ms time scale it takes to release the applied pressure (Fig. 3a).

Fig. 4b displays the average λ as a function of MW for all polymeric solutions. Also displayed in Fig. 4b is the predicted scaling of polymeric solutions by the well-known finite extensibility nonlinear elastic (FENE) constitutive model, $\lambda \sim MW^{2/3}$.[2,22] We note that there are discrepancies between the experimental data and the fitting for small MW. This is likely caused by the limitations of the model; for instance it assumes a mean relaxation time, while real polymeric solutions have a spectrum of relaxation times. We also characterize the fluid with a single relaxation time, yet the technique used here measures the longest relaxation time, not the mean. Therefore, the differences between our measurements and the FENE model prediction in the scaling of λ are expected. In addition, we are unable to measure λ of the MW 1.5×10^3 PAA solution.

Finally, we compare the values of λ obtained using the microfluidic device to results obtained using a commercially available rheometer.[7] The values of λ using the cone-and-plate rheometer for the MW 1.0×10^4, 1.0×10^6 and 1.8×10^7 PAA solutions are 0.009 s, 0.06 s, and 0.45 s, respectively.[7] The value of λ for the MW 1.5×10^3 PAA solution could not be reliably measured in the macroscopic rheometer due to lack of sensitivity in measuring the fluid first normal stress difference (N_1). Differences between the measurements could be due to polymer MW polydispersity as well as the fact that these two techniques probe the sample in different ways, resulting in changes between the observable time scales. Nonetheless, the data presented in Fig. 4 are very close to the values obtained with the commercial rheometer. These results indicate that microfluidics can be reliably used to obtain creep and relaxation data of complex, viscoelastic fluids.

We have demonstrated the feasibility of measuring the fluid relaxation and creep recovery in a microfluidic device. We measured relaxation times as low as 20 ms at small strain, ranging from 0.01 to 10. The relaxation data are consistent with measurements in commercial rheometers[7] and with a well-known viscoelastic constitutive model, namely the FENE model.[2,22] The ability to measure small time scales at low strains in fluids can be a challenge, especially in many biological fluids of interest such as blood plasma, DNA solutions, and fluids containing proteins. However, the method proposed here provides an inexpensive method to observe material relaxation and perform time-dependent rheological measurements, particularly small time scales at low strains, to complement traditional macroscopic rheometry.

Acknowledgements

The authors thank D.J. Durian and X.N. Shen for helpful discussions as well as P. Szczesniak and H. Bau for assistance with the experimental setup. This work is supported by Penn NSF MRSEC (DMR-1120901).

References

1 R. Larson, *The Structure and Rheology of Complex Fluids*, Oxford University Press, New York, 1999.
2 R. Bird, *Dynamics of Polymeric Liquids*, Wiley, 1987, vol. 1.
3 S. Haward, T. Ober, M. Oliveira, M. Alves and G. McKinley, *Soft Matter*, 2012, **8**, 536–555.
4 V. Chikkadi, G. Wegdam, D. Bonn, B. Nienhuis and P. Schall, *Phys. Rev. Lett.*, 2011, **107**, 198303.
5 P. Sousa, F. Pinho, M. Oliveira and M. Alves, *Biomicrofluidics*, 2011, **5**, 014108.
6 G. Juarez and P. Arratia, *Soft Matter*, 2011, **7**, 9444–9452.
7 P. Arratia, L. Cramer, J. Gollub and D. Durian, *New J. Phys.*, 2009, **11**, 115006.
8 L. Rodd, T. Scott and D. Boger, *J. Non-Newtonian Fluid Mech.*, 2005, **129**, 1–22.
9 A. Groisman, M. Enzelberger and S. Quake, *Science*, 2003, **300**, 955–958.
10 D. Smith and S. Chu, *Science*, 1998, **281**, 1335–1340.
11 V. Tirtaatmadja, G. McKinley and J. Cooper-White, *Phys. Fluids*, 2006, **18**, 043101.
12 K. Nordstorm, P. Arratia, E. Verneuil, A. Basu, Z. Zhang, A. Yodh, J. Gollub and D. Durian, *Phys. Rev. Lett.*, 2010, **105**, 175701.
13 C. Pipe, T. Majmudar and G. McKinley, *Rheol. Acta*, 2008, **47**, 244107.
14 G. Degre, P. Joseph, P. Tabeling, S. Lerouge, M. Cloitre and A. Ajdari, *Appl. Phys. Lett.*, 2006, **89**, 024104.
15 G. McKinley and T. Sridhar, *Annu. Rev. Fluid Mech.*, 2002, **34**, 375–415.
16 S. Haward, J. Odell, M. Berry and T. Hall, *Rheol. Acta*, 2011, **50**, 869–879.
17 D. Hohne, J. Younger and M. Solomon, *Langmuir*, 2009, **25**, 7743–7751.
18 S. Teh, R. Line, L. Hung and A. Lee, *Lab Chip*, 2008, **8**, 198–220.
19 M. Unger, H. Chou, T. Thorsen, A. Scherer and S. Quake, *Science*, 2000, **288**, 113–116.
20 M. Wang, E. Tu, D. Raymond, J. Yang, H. Zhang, N. Hagen, B. Dees, E. Mercer, A. Forster, I. Kariv, J. Marchand and W. Butler, *Nat. Biotechnol.*, 2005, **23**, 83–87.
21 L. Huang, E. Cox, R. Austin and J. Sturm, *Science*, 2004, **304**, 987–990.
22 A. Peterlin, *J. Polym. Sci., Part B: Polym. Lett.*, 1966, **4**, 287–291.